Study and comparison of various speeds during taxiing operations at Orly airport

SESAR Exercise

Case Study - Orly Airport

Author : Émilien FOISSOTTE
Reviewed by : Pierre JOUNIAUX

Machine Learning and Research Department - Safety Line

May 2022

Reviewed on 19th May

Contents

List of Figures 2

1 Introduction 3
- 1.1 Contextualization and presentation of case study's objectives . . . 3
- 1.2 Perspective of achievements . . . 3

2 Practical Case - August 2021 Study 4
- 2.1 Case Study . . . 4
  - 2.1.1 Presentation and achievements of the preliminary work . . . 4
  - 2.1.2 Geo-Spatial Distribution of Taxiing Speeds . . . 6
- 2.2 Defining a scale to map speed divergence and over-consumption . . . 9
  - 2.2.1 At the level of a single trajectory . . . 9
  - 2.2.2 At the level of the whole platefrom . . . 11
- 2.3 Conclusion . . . 15
  - 2.3.1 Speed recommendation savings expectations . . . 15
  - 2.3.2 Trajectory recommendation savings expectations . . . 16

Bibliography 18

List of Figures

2.1 Taxiing graph obtain by querying Open Street Map API 5
2.2 Process of fast Map Matching Algorithm 5
2.3 Distribution of takeoff taxiing speeds in West configuration 6
2.4 Distribution of takeoff taxiing speeds in East configuration 7
2.5 Distribution of landing taxiing speeds in West configuration 7
2.6 Distribution of landing taxiing speeds in East configuration 8
2.7 Fuel consumption for different engine rate 10
2.8 Differents speed profile 11
2.9 Cartography of the divergence to the recommended speeds on West landings 12
2.10 Cartography of the divergence to the recommended speeds on East landings 12
2.11 Cartography of the divergence to the recommended speeds on West takeoffs 13
2.12 Cartography of the divergence to the recommended speeds on East takeoffs 14
2.13 Distribution of speed differences between QAR data and recommendation 15
2.14 Distribution of simulated speed differences between QAR data after speed recommendation policies 16

Chapter 1

Introduction

1.1 Contextualization and presentation of case study's objectives

This case study is conducted to study various element of taxiing operations at Orly airport, especially the choice of the speed for an aircraft to move on the platform.

The context of this case study addresses an operational need of APOC[1] as part of the airport platform, to study various taxiing speed and quantify the fuel consumption, and therefore the amount of CO_2 and NO_x generetad at this speed.

1. The first objective is to study the overall distributions of taxiing speeds on the airport given a specific configuration and a specific type of movement. The main purpose of this objective is to identify recurring pattern in the actual speeds.

2. Another objective of the study is also to study the impact of an over-representation of high speeds or slow speeds on taxiing trajectories in order to quantify the environnemental consequences of a shift between speeds recommended and speeds actually selected to proceed taxiing operations.

1.2 Perspective of achievements

In order to fullfill theses various objectives, a simple methodology will be presented and conducted to present our conclusions.

The first part of the study will be to proceed to a map-matching of a set of trajectories on a graph of the Orly platform. Once all trajectories are map-matched to edges on a graph, a study of the distribution of the taxiing speeds will be done to analyze the significant patterns of taxiing speeds.

The second part of the study will consist in the analysis of QAR[2] data to proceed to a mapping of taxiing speed and engine rates, in order to quantify the impact of a chosen speed during a taxiing operation on environmental markers (fuel consumption, gaseous emissions of CO_2 and NO_x emitted).

[1] Airport Operation Center
[2] Quick Access Recorder

Chapter 2

Practical Case - August 2021 Study

2.1 Case Study

2.1.1 Presentation and achievements of the preliminary work

In order to obtain a taxiing graph of the Orly platform, several methods exist:

- **1 - Description geofile** - Retrieve a description file of the taxiways and extract the GPS coordinates.
- **2 - Image processing** - Use image processing and topological graph refinement methods from a radar data stream.
- **3 - OSM API** Query objects stored in the APIs of Open Source geographic data repositories (Open Street Map) and process them to extract a graph.

As methodology N°2 was already done on the previous case study (Gaseous Emission on Runway Inspection), we could analyze the resulting graph obtained and conclude if the topological quality is sufficient to proceed with this graph during this case study. The resulting graph was precise enough to conduct a comparative analysis with the methodology used in the case study on runway inspection.

However, due to partially inacurrate edge geometry, the resulting graph of the previous case study cannot be safely used to proceed to the map matching, the accuracy of the geometry is not sufficient for the map-matching algorithm and could lead to errors (and significant errors during this process). Due to this restriction and the crucial importance of map-matching step in our algorithm to obtain precise edge topology and their relative distribution of speeds, we changed our method to retrieve a runways and taxiways graph.

To obtain a new taxiing graph with method n°3, queries have been made to Nominatim[1] API following methodology described in (Boeing, 2017).

A precomputed Upper Bounded Origin Destination Table(UBOT), as referecend by (Yang and Gidofalvi, 2018) in the **Fast Map Matching** methodology has been obtained by querying the obtained graph displayed in 2.1. A UBOT consist in a matrix which contains for each row the shortest path to reach an orign node to a destination node. The whole concept of Map Maptching is described in figure 2.2 extracted from (Yang and Gidofalvi, 2018)

[1] OpenStreetMap API to query geolocation objects

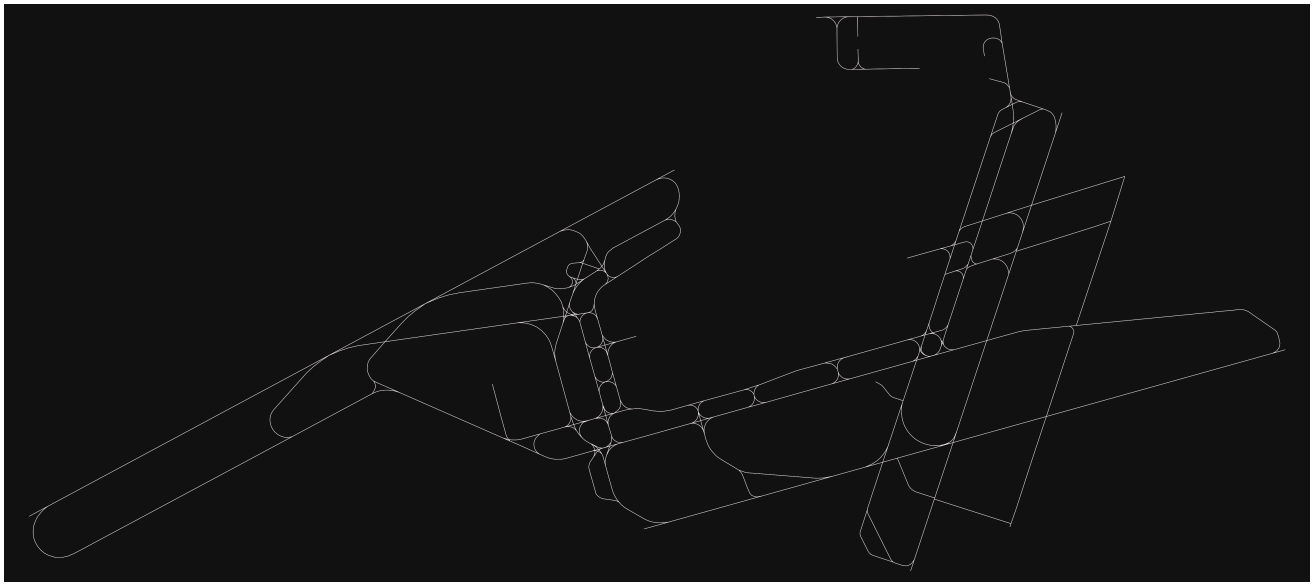

Figure 2.1: Taxiing graph obtain by querying Open Street Map API

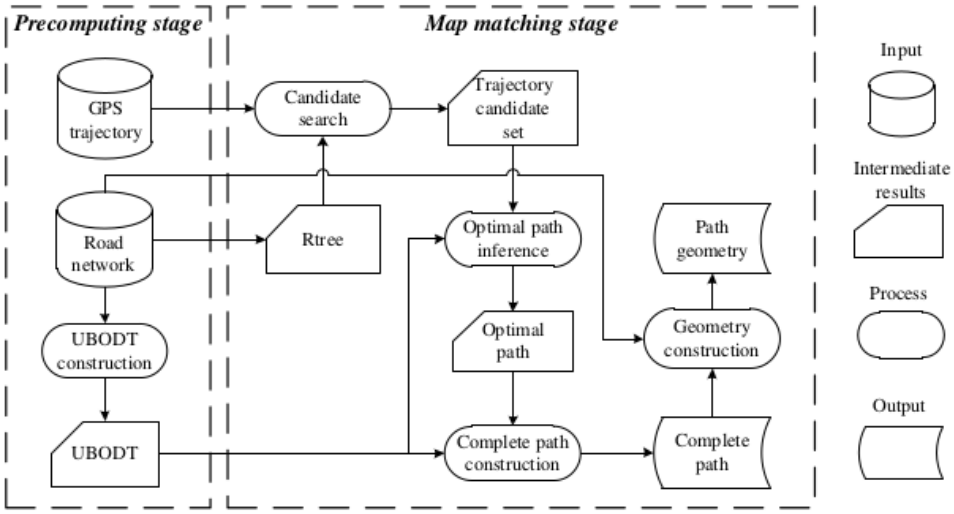

Figure 2.2: Process of fast Map Matching Algorithm

2.1.2 Geo-Spatial Distribution of Taxiing Speeds

A map matching of all trajectories observed with turbofan engines aircraft has been done to obtain a geo-spatial graph of the taxiing speed distribution, over the period of August 2021 (from the 1st to the 31th of the month). All value of speed under 1 mps is considered to be a stop and therefore excluded from the set of speeds observed. The resulting graph is constituted of edges weighted by the average speed observed on the edge, given a particular movement (take-off or landing) and a particular configuration (West or East).

Takeoffs - West

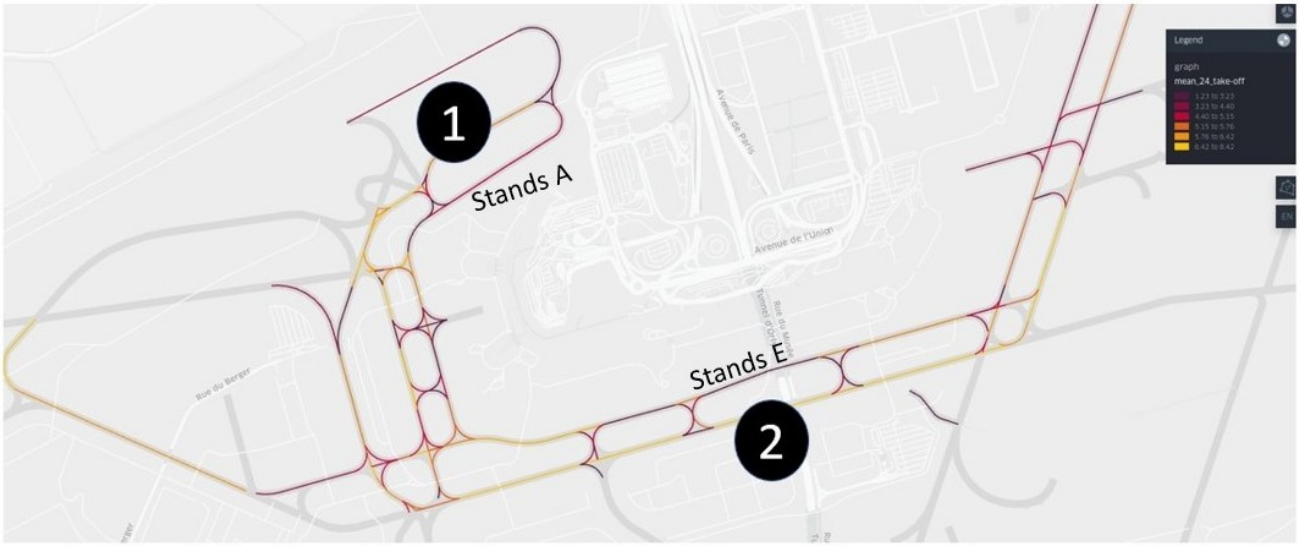

Figure 2.3: Distribution of takeoff taxiing speeds in West configuration

It can be observed that in average speeds are higher on specific straight part of taxiways and is not symmetrical.

- On the spot number 1, taxiing speeds far away from stands on the nothern part of the plateform, in front of the stands A01 to A22, are higher than the section near closest to the stands. A difference of more than 1 mps can be observed between theses taxiways, with a standard deviation of 1 mps for each edge considered.
- A similar situation can be observed on the spot number 2, where the median speed considered is around 7 mps whereas near the stands E01 to E20, the median speed drops to values around 2 mps.

Main differences observed between configuration are located in regions where the configuration implies that aircraft are evolving on the taxiway differently, for instance near the runway thresholds. However, same distributions can be found where sharp turns are observed (speeds on these section varies from 2 mps to a maximum of 4 mps) whilst where trajectories are following a straight path, the speed can easily reach values of 7 mps.

Takeoffs - East

Figure 2.4: Distribution of takeoff taxiing speeds in East configuration

Landings - West

Figure 2.5: Distribution of landing taxiing speeds in West configuration

Landings - East

Figure 2.6: Distribution of landing taxiing speeds in East configuration

The main differences between theses distribtions are located near the exit of the runway, higher speeds can be observed neart those exit points of the runway.

2.2 Defining a scale to map speed divergence and over-consumption

2.2.1 At the level of a single trajectory

The main purpose of this section is to study the optimal speed recommendation along a single trajectory and explain the behind the scenes of the recommended trajectories.

First of all, the first step has been to extract the median speed observed on the platform in order to provide an acceptable and physically rollable recommendation of speed along an edge of the taxiway graph. This speed is the target to achieve by the pilot on the edge.

Along a taxiway trajectory, the contribution to the fuel consumption, and therefore to the emission produced, can be expressed and simplified by laws describing the functionning of the turbofans during taxiway operation.

The fuel consummed during operation can be described by 2.1. The fuel consumed during an operation is expressed by mulitplying the duration of the operation to the observed fuel flow of this operation. The observed fuel flow depends directly from the engine rate observed at each instant of the operation, following the OACI methodology, by interpolating engine rates, N_1 and fuel flow on 4 functioning point of the turbofan engines, at idle point (7%), approach (30%), climb (80%) and lastly take-off (100%). However, as shown in QAR data, the typical engine rates we selected to conduct this modelization are between 20% and 40%.

$$fuelconsumption = time * fuelflow(N_1) * numberofengines \tag{2.1}$$

On a specific edge, three variables have to be defined in order to set up the modelization, the length of the edge, and the maximum speed which can be reached on the edge and finally the the starting speed on the edge. Given theses information, an idealistic speed profile can be determined in order to minimize the fuel consumption, per aircraft and per edge.

Given the equation to determine the fuel consumption we modelize an increase of acceleration due to an increase of engine rate with the following equation (thus we do not take in account inertia here, considering the effect of engine rate increase are immediate, as consequence of this delay are neglicatble on overall fuel consumption). The modelization of increase in acceleration is expressed in equation 2.2, where N_1 is expressed in percentage. The main purpose is to observe an equalization of resisting force when the N_1 equals 20%, the resulting acceleration of the aircraft is null and moves at constant speed. With an engine rate of N_1 at 40%, the resulting longitudinal acceleration observed in QAR data is around 0.1 G (one G of accereration equals around $9.81 m/s^{-2}$)

$$acceleration_{m/s} = 0.04905 * N_1 - 0.981 \tag{2.2}$$

Using an example with an edge of a length of 110 meters on the graph where the maximum speed reachable is 54 km/h, the initial speed is 18 km/h, where the taxiing operation is done with a Boieng 737 (equipped of 2 CFM56-7B22), the consumption given the engine rate during the acceleration phase are shown on fig 2.7.

The movement have been sperated in 3 cases:

- The engine rate is selected to do not counter resistance to movement and is set exactly at 20% in order to do not accelerate. Thus, the movement is done at constant speed, the initial one. The profile is displayed on figure 2.8a
- The engine rate is selected above 20%, therefore an acceleration is observed. However, the maximum speed is not reached on the edge, then the engine rate is constantly set to this value and the acceleration is constant over the whole edge. The profile is presented on figure 2.8b
- The engine rate is selected again above 20%, however, the acceleration is so high that the maximum speed is reached before the end of the edge. Then, we observe a section of constant acceleration, given by the engine rate selected and when the maximum speed is reached, the engine rate returns to a value of

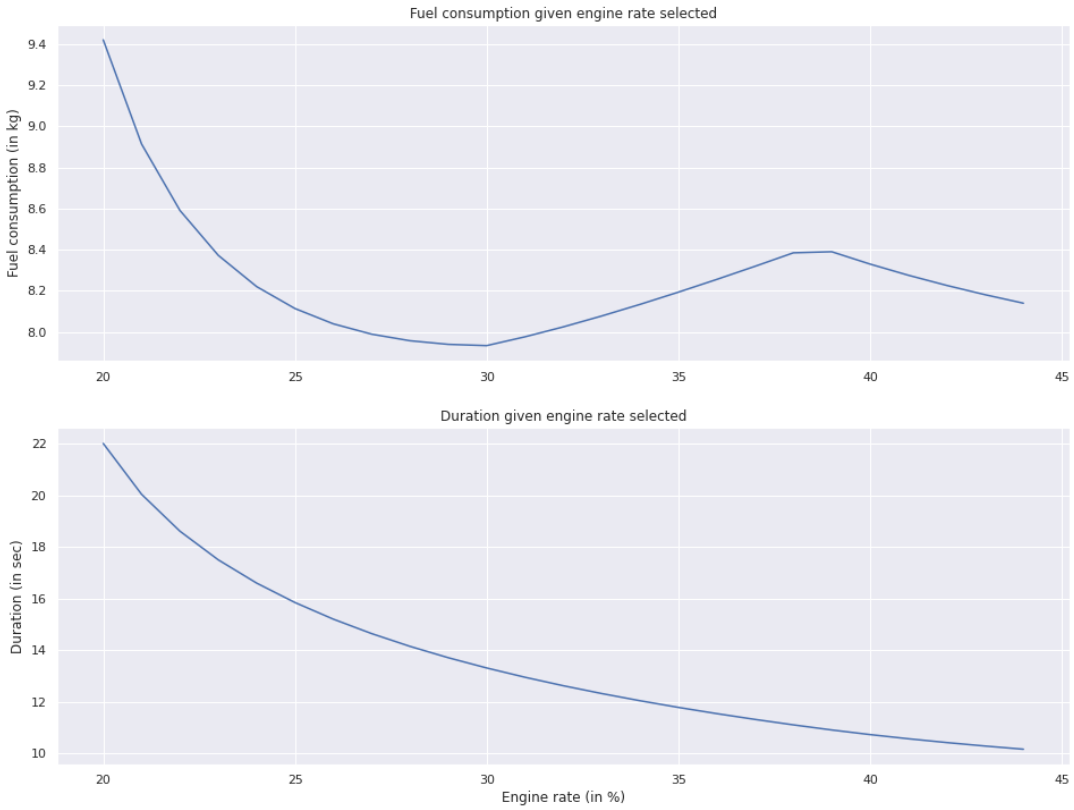

Figure 2.7: Fuel consumption for different engine rate

20% to equalize the resistance to the movement only and give an acceleration of zero. The first section is in blue on figure 2.8a and the constant speed part in yellow.

On the situation presented on figure 2.7, the ideal engine rate given the caracteristics of the edge and the topology of the modelized path is a percentage of 30% for the engine rate.

Using different parameters during taxiway operations on this modelized edge would cause overconsumption of fuel, and therefore an emission of gaseous emissions maximized compared to this optimal situation. This overconsumption can be quantified, in function of the length of the edge. Using the parameters previously used, we can determine the following values :

- Using a engine rate above the optimum value, for instance, an engine rate of 7% above the optimum value, generating a speed difference of 5 km/h above the optimum value over the edge, the fuel consumption is increased by 4.9%.
- Using an engine rate over the edge below the optimum value, for instance an engine rate of 7% percents below the optimum value generating a speed difference of 7 km/h below the optimum speed for the edge will increase the fuel consumption by 5.5 %.

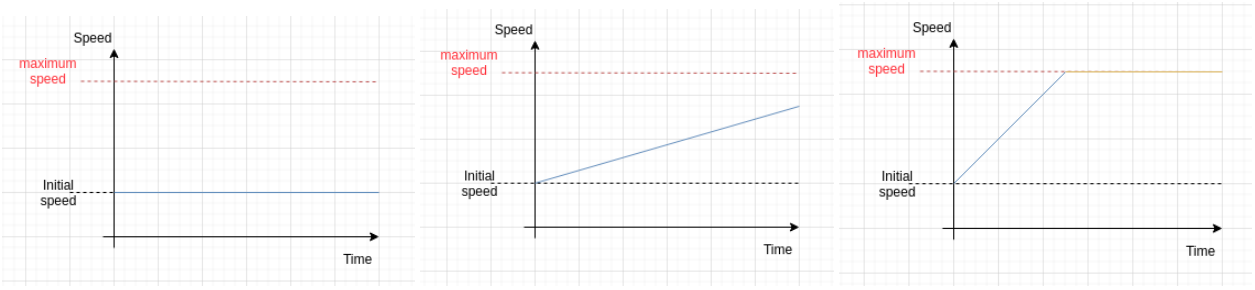

(a) Profile without acceleration (b) Profile with smooth acceleration (c) Profile with firm acceleration

Figure 2.8: Differents speed profile

2.2.2 At the level of the whole platefrom

400000 single point of QAR data over the month of August from 1237 flights has been map-matched, analyzed and compared to the recommended speeds provided and aggregated to display these maps.

The formula used to display divergence between recommended speeds and the observed ones is written on equation 2.3. Units in use here are meter per seconds.

$$speed_{difference} = speed_{observed} - speed_{reference} \tag{2.3}$$

This means that an observed value which is higher than recommendation will be display as an high value and therefore mapped to a high value of speed difference. These typical values are displayed as red dots on cartography.

On the contrary, observed speeds values from the QAR data during taxiway which are below recommended speeds will be display as negative values of speed difference. Theses values are displayed as green dots on the map.

Landings - West

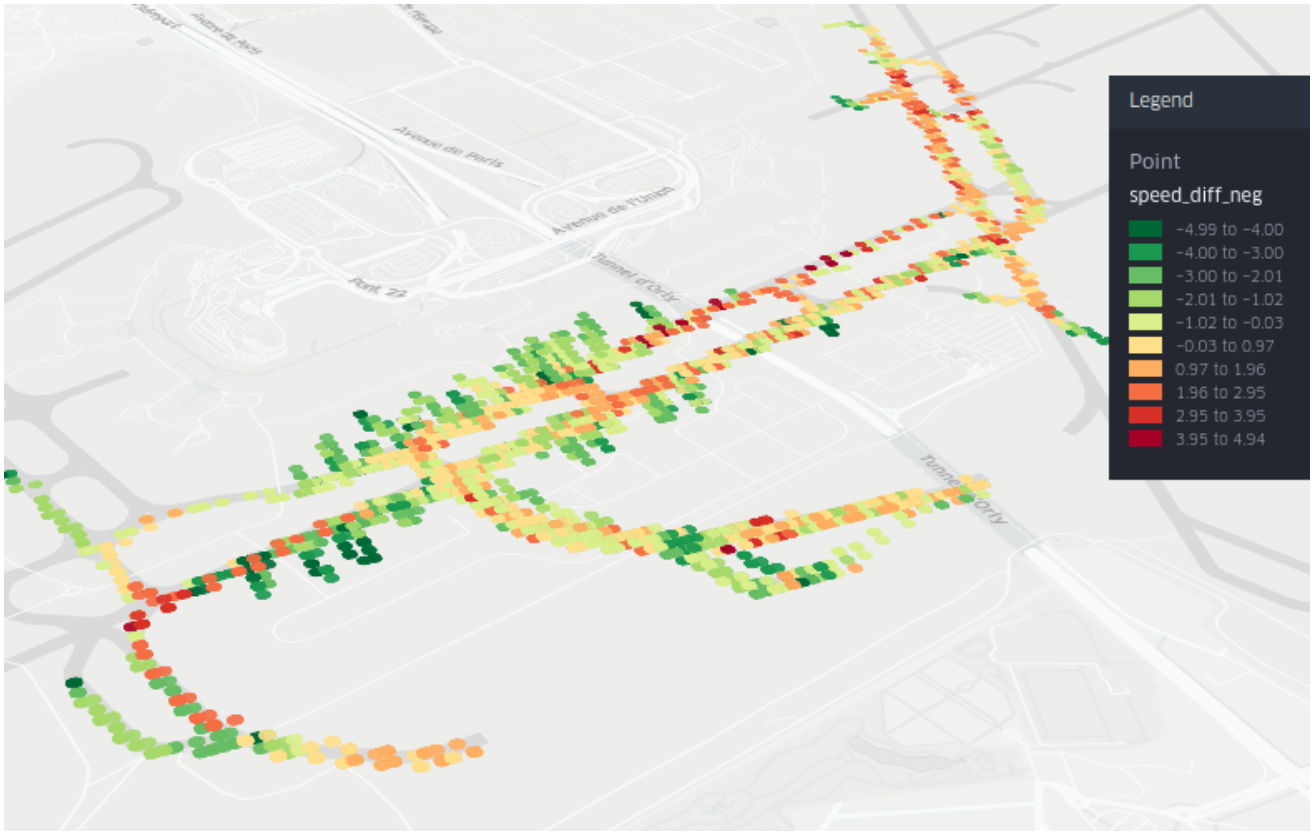

Figure 2.9: Cartography of the divergence to the recommended speeds on West landings

Landings - East

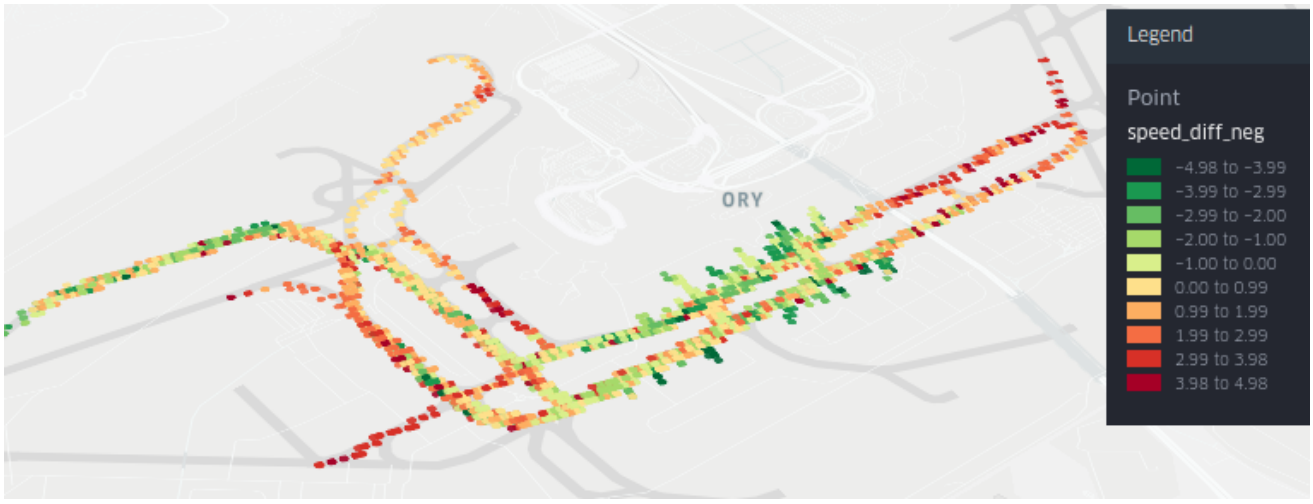

Figure 2.10: Cartography of the divergence to the recommended speeds on East landings

Landings recurring patterns

On the landings cartography shown on 2.10 and 2.9, lower speeds than recommended ones are usually observed near stands, where the aircraft might be finished his pushback, and therefore is moving at slow speed. Highest

speeds can be observed mainly during straight taxiway sections.

Take-offs - West

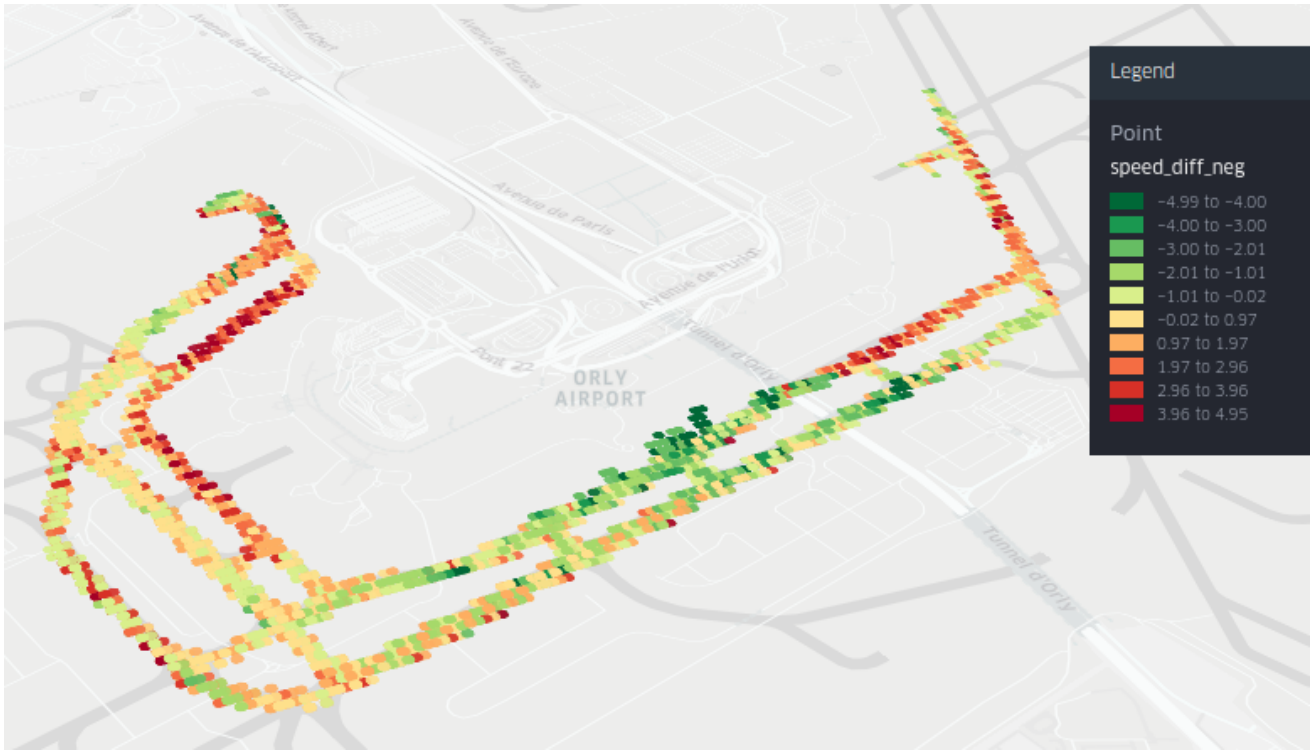

Figure 2.11: Cartography of the divergence to the recommended speeds on West takeoffs

Take-offs - East

Figure 2.12: Cartography of the divergence to the recommended speeds on East takeoffs

On the takeoffs cartography shown on 2.12 and 2.11, higher speeds differences are distributed over straight portion also of the runway graph. On the contrary, low speed differences, indicating that observed speeds are lower than the recommended ones are distributed near stands, on the southern part of the platform.

Another spot of high speed differences is located near runway threholds where some aircrafts tends to accelerate on theses runway sections, which generate amount of speeds beyond average taxiing values.

2.3 Conclusion

2.3.1 Speed recommendation savings expectations

To conclude, we analyzed the QAR over the August 2021 period to estimate the potential savings of an implementation of taxiing and path recommendation in term of CO_2 and fuel saved.

Concerning the speed recommendation the speed difference observed between speed recommendation and the speed observed in QAR data has a variance of 3.73. We could assume that recommend speeds could lead to a minimization of this standard deviation, and therefore a more centric distribution of speeds difference.

On the current observation, we could assume that distribution of speed difference along trajectories follow a Gaussian curve with a standard deviation of 1.93, as 68% of values of speed differences are between $]-5.1, 8.7[$ km/h, as shown on fig 2.13, where the estimation of the kernel density is represented with the blue line plot and the red line shows the modelization with a Gaussian distribution curve, where $\mu = 0.5$ and $\sigma = 1.93$.

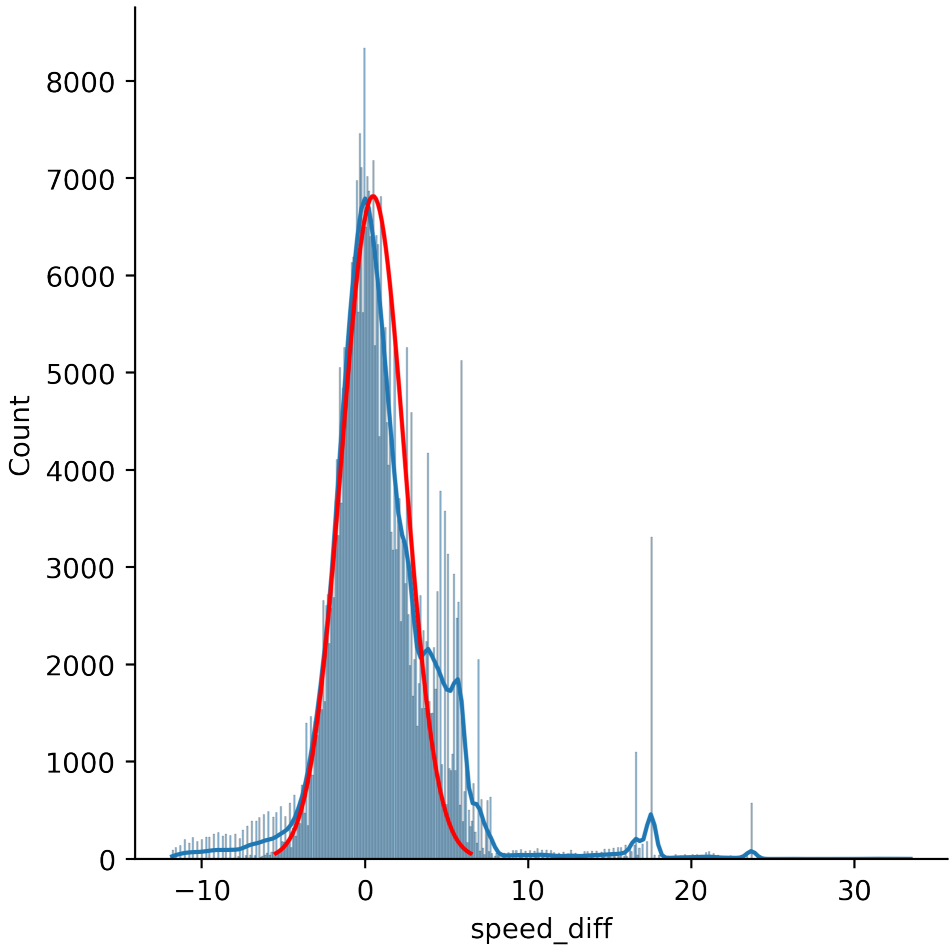

Figure 2.13: Distribution of speed differences between QAR data and recommendation

The contribution to divergence, using a linear law to interpolate previous result from overconsumption on speed values below recommendation and speed values over recommendation can be expressed with such equation 2.4, where SD stands for *speed difference* in km/h. Be careful here, as the exercise has been done for a specific edge on a specific setting for initial speeds values, with a specific consumption law for turbofans engine, the value computed here is only an estimate of potential savings.

$$overconsumption(\%) = f(SD) = \begin{cases} 0.78 \times SD & SD \leq 0 \\ 0.98 \times SD & SD \geq 0 \end{cases} \tag{2.4}$$

Hence by computing an integral of the probability density function of speed difference distribution multiplied by its contribution to increase of consumption of the actual situation, as per following equation 2.5 we find a value of overconsumption of 4.9%.

$$overconsumption(\%) = \int_{0.01_{eq}}^{0.99_{eq}} \frac{1}{\sigma\sqrt{2\pi}} e^{\frac{(x-\mu)^2}{2\times\sigma^2}} dx \tag{2.5}$$

By considering we could reduce the standard deviation of this distribution, by promoting speed recommendation to pilot, we could expect that now the new standard deviation is divided by 3, meaning that 63% of values between $]-4,4[$ km/h, represented as the red line plot on the figure 2.14

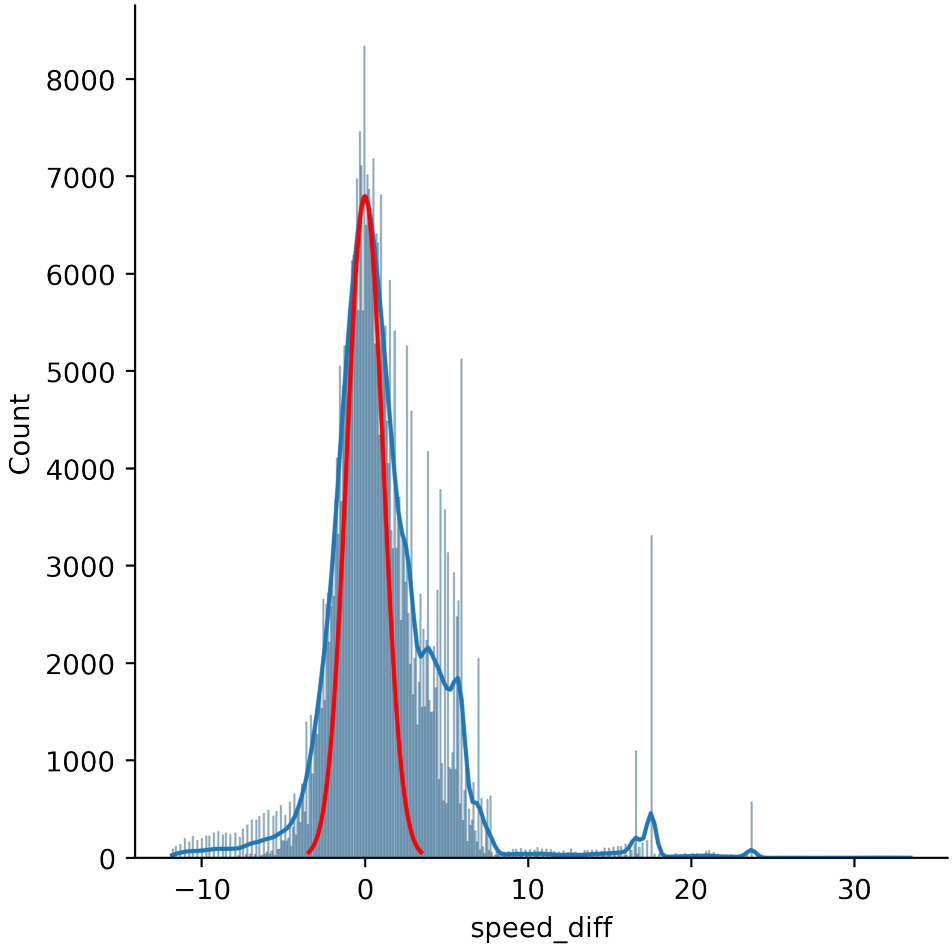

Figure 2.14: Distribution of simulated speed differences between QAR data after speed recommendation policies

With this new distribution, overconsumption is reduced to only 2.6% of total fuel consumption, hence promoting theses types of taxiing policies could lead to a reduction of 2.3 % of taxiing fuel consumption.

Thus on a daily basis, we could expect savings of 1490 kg of fuel, contributing to reduce CO_2 emissions of 4694 kg.

2.3.2 Trajectory recommendation savings expectations

On the aspect of trajectory recommendation, we can observe first of all that on average, independantly from a specific configuration or a an aircraft type, a consumption of 162 kg of fuel is observed in average for the most

fuel saving path. In West configurations the 3rd path overconsume 212 kg of fuel, whereas in East configuration, the 3rd path consume 180 kg of fuel. On a basis of 400 movement per day, we could expect that in average, without any information the 3rd path is chosen whereas now, the first path is choosen.

- **West :** Fuel and CO_2 emissions savings of 30% per movement, which could lead to saving of around 20 tonnes of fuel, thus equivalent to 63 tonnes of CO_2
- **East :** Fuel and CO_2 emissions savings of 13.5% per movement, which could lead to saving of around 8.8 tonnes of fuel, thus equivalent to around 28 tonnes of CO_2

Bibliography

G. Boeing. Osmnx: New methods for acquiring, constructing, analyzing, and visualizing complex street networks. *Computers, Environment and Urban Systems*, 65:126–139, 2017.

C. Yang and G. Gidofalvi. Fast map matching, an algorithm integrating hidden markov model with precomputation. *International Journal of Geographical Information Science*, 32(3):547–570, 2018. doi: 10.1080/13658816.2017.1400548. URL https://doi.org/10.1080/13658816.2017.1400548.